

Observational $H(z)$ Data and Cosmological Models

Hao Wei^{1,*} and Shuang Nan Zhang^{1,2,3}

¹*Department of Physics and Tsinghua Center for Astrophysics,
Tsinghua University, Beijing 100084, China*

²*Key Laboratory of Particle Astrophysics, Institute of High Energy Physics,
Chinese Academy of Sciences, Beijing 100049, China*

³*Physics Department, University of Alabama in Huntsville, Huntsville, AL 35899, USA*

Abstract

In this work, we confront ten cosmological models with observational $H(z)$ data. The possible interaction between dark energy and dust matter is allowed in some of these models. Also, we consider the possibility of (effective) equation-of-state parameter (EoS) crossing -1 . We find that the best models have an oscillating feature for both $H(z)$ and EoS, with the EoS crossing -1 around redshift $z \sim 1.5$.

PACS numbers: 95.36.+x, 98.80.Es, 98.80.-k

* email address: haowei@mail.tsinghua.edu.cn

1 Introduction

A lot of cosmological observations, such as SNe Ia [1, 2], WMAP [3], SDSS [4], Chandra X-ray Observatory [5] etc., find that our universe is experiencing an accelerated expansion. These results also suggest that our universe is spatially flat, and consists of about 70% dark energy with negative pressure, 30% dust matter (cold dark matters plus baryons), and negligible radiation. Dark energy study has been one of the most active fields in modern cosmology [6].

In the past years, many cosmological models are constructed to interpret the present accelerated expansion. One of the important tasks is to confront them with observational data. The most frequent method to constrain the model parameters is fitting them to the luminosity distance

$$d_L(z) = (1+z) \int_0^z \frac{d\tilde{z}}{H(\tilde{z})}, \quad (1)$$

which is an integral of Hubble parameter $H \equiv \dot{a}/a$, where $a = (1+z)^{-1}$ is the scale factor (z is the redshift); a dot denotes the derivative with respect to cosmic time t . In this work, we use the observational $H(z)$ data directly, rather than the luminosity distance $d_L(z)$. The observational $H(z)$ data are based on differential ages of the oldest galaxies [7]. In [8], Jimenez *et al.* obtained an independent estimate for the Hubble constant by the method developed in [7], and used it to constraint the equation-of-state parameter (EoS) of dark energy. The Hubble parameter depends on the differential age as a function of redshift z in the form

$$H(z) = -\frac{1}{1+z} \frac{dz}{dt}. \quad (2)$$

Therefore, a determination of dz/dt directly measures $H(z)$ [9]. By using the differential ages of passively evolving galaxies determined from the Gemini Deep Deep Survey (GDDS) [10] and archival data [11], Simon *et al.* determined $H(z)$ in the range $0 \lesssim z \lesssim 1.8$ [9]. The observational $H(z)$ data from [9] are given in Table 1 and shown in Figs. 2–5.

z	0.09	0.17	0.27	0.40	0.88	1.30	1.43	1.53	1.75
$H(z)$ (km s ⁻¹ Mpc ⁻¹)	69	83	70	87	117	168	177	140	202
1σ uncertainty	± 12	± 8.3	± 14	± 17.4	± 23.4	± 13.4	± 14.2	± 14	± 40.4

Table 1: The observational $H(z)$ data [8, 9] (see [15] also).

These observational $H(z)$ data have been used to constrain the dark energy potential and its redshift dependence by Simon *et al.* in [9]. Yi and Zhang used them to constrain the parameters of holographic dark energy model in [12]. Some relevant works also include [13, 14]. Recently, in [15], Samushia and Ratra have used these observational $H(z)$ data to constrain the parameters of Λ CDM, XCDM and ϕ CDM models. In this work, we will revisit these observational $H(z)$ data and compare them with some cosmological models.

By looking carefully on the observational $H(z)$ data given in Table 1 and shown in Figs. 2–5, we notice that two data points near $z \sim 1.5$ and 0.3 are very special. They deviate from the main trend and dip sharply, especially the one near $z \sim 1.5$; the $H(z)$ decreases and then increases around them. This hints that the effective EoS crossed -1 there. This possibility has not been discussed in previous works (e.g. [12, 15]). In the present work, we will seriously explore this possibility.

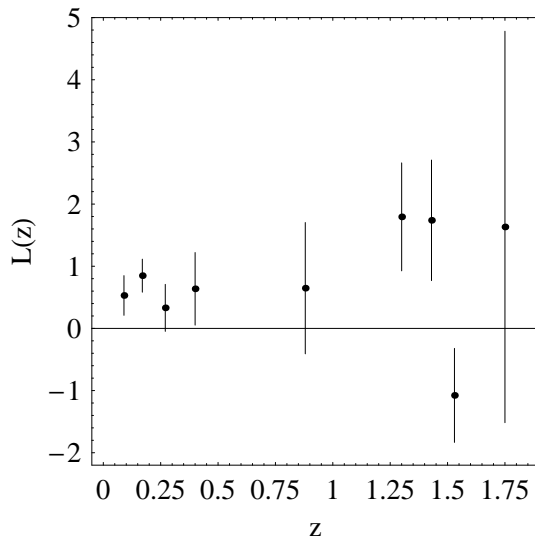


Figure 1: The quantity $L(z) \equiv H^2(z)/H_0^2 - \Omega_{m0}(1+z)^3$ versus redshift z , for the fiducial parameters $H_0 = 72 \text{ km s}^{-1} \text{ Mpc}^{-1}$ and $\Omega_{m0} = 0.3$.

On the other hand, we also consider the possible interaction between dark energy and dust matter. This is inspired by the data point near $z \sim 1.5$, which dips so sharply and stays clearly outside of the best-fit of the Λ CDM, XCDM and ϕ CDM models studied in [15]. In Fig. 1, we show the quantity $L(z) \equiv H^2(z)/H_0^2 - \Omega_{m0}(1+z)^3$ versus redshift z , which is associated with the fractional energy density of dark energy, for the fiducial parameters $H_0 = 72 \text{ km s}^{-1} \text{ Mpc}^{-1}$ and $\Omega_{m0} = 0.3$, where the subscript “0” indicates the present value of the corresponding quantity. It is easy to see that the fractional energy density of dark energy of the point near $z \sim 1.5$ is negative (beyond 1σ significance). To avoid this, one can decrease the corresponding Ω_{m0} or make the matter decrease with the expansion of our universe slower than a^{-3} . Inspired by this, it is natural to consider the possibility of exchanging energy between dark energy and dust matter through interaction.

We assume that dark energy and dust matter exchange energy through interaction term C , namely

$$\dot{\rho}_{de} + 3H(\rho_{de} + p_{de}) = -C, \quad (3)$$

$$\dot{\rho}_m + 3H\rho_m = C, \quad (4)$$

which preserves the total energy conservation equation $\dot{\rho}_{tot} + 3H(\rho_{tot} + p_{tot}) = 0$. The interaction forms extensively considered in the literature (see [16, 17, 18, 19, 20, 21, 22, 23, 24, 25, 26, 39] for instance) are

$$C \propto H\rho_m, H\rho_{tot}, H\rho_{de}, \kappa\rho_m\dot{\phi}, \dots$$

In this work, we consider the simplest case for convenience, i.e.

$$C = 3\alpha H\rho_m, \quad (5)$$

where α is a dimensionless constant. Combining Eqs. (4) and (5), it is easy to get

$$\rho_m = \rho_{m0} a^{-3(1-\alpha)} = \rho_{m0}(1+z)^{3(1-\alpha)}. \quad (6)$$

In the following sections, we will compare the observational $H(z)$ data with some cosmological models with/without interaction between dark energy and dust matter. We consider a spatially flat FRW universe

throughout. We adopt the prior $H_0 = 72 \text{ km s}^{-1} \text{ Mpc}^{-1}$, which is exactly the median value of the result from the Hubble Space Telescope (HST) key project [27], and is also well consistent with the one from WMAP 3-year result [3]. Since there are only 9 observational $H(z)$ data points and their errors are fairly large, they cannot severely constrain model parameters alone. We perform a χ^2 analysis and compare the cosmological models to find out the one which catches the main features of the observational $H(z)$ data. We determine the best-fit values for the model parameters by minimizing

$$\chi^2(\text{parameters}) = \sum_{i=1}^9 \frac{[H_{\text{mod}}(\text{parameters}; z_i) - H_{\text{obs}}(z_i)]^2}{\sigma^2(z_i)}, \quad (7)$$

where H_{mod} is the predicted value for the Hubble parameter in the assumed model, H_{obs} is the observed value, σ is the corresponding 1σ uncertainty, and the summation is over the 9 observational $H(z)$ data points at redshift z_i .

2 Λ CDM and XCDM models without/with interaction

In the spatially flat Λ CDM model, the Hubble parameter is given by

$$H(z) = H_0 \sqrt{\Omega_{m0}(1+z)^3 + (1 - \Omega_{m0})}, \quad (8)$$

where $\Omega_{m0} \equiv \kappa^2 \rho_{m0} / (3H_0^2)$ is the present fractional energy density of the dust matter, and $\kappa^2 \equiv 8\pi G$. By minimizing the corresponding χ^2 , we find that the best-fit value for model parameter is $\Omega_{m0} = 0.302$, while $\chi_{\text{min}}^2 = 9.04$ and $\chi_{\text{min}}^2 / \text{dof} = 1.13$, where *dof* is the degree of freedom.

Then, we consider the interacting Λ CDM model (Int Λ CDM). In this case, Eq. (3) becomes

$$\dot{\rho}_\Lambda = -3\alpha H \rho_m. \quad (9)$$

By using Eq. (6), it is easy to find

$$\rho_\Lambda = \frac{\alpha}{1-\alpha} \rho_{m0} a^{-3(1-\alpha)} + \text{const.} \quad (10)$$

where *const.* is an integral constant. Inserting into the Friedmann equation $H^2 = \kappa^2(\rho_m + \rho_\Lambda)/3$ and requiring $H(z=0) = H_0$, one can determine the integral constant. Finally, in the Int Λ CDM model, the Hubble parameter is given by

$$H(z) = H_0 \sqrt{\frac{\Omega_{m0}}{1-\alpha}(1+z)^{3(1-\alpha)} + \left(1 - \frac{\Omega_{m0}}{1-\alpha}\right)} \quad (11)$$

By minimizing the corresponding χ^2 , we find that the best-fit values for model parameters are $\Omega_{m0} = 0.386$ and $\alpha = 0.138$, while $\chi_{\text{min}}^2 = 8.89$ and $\chi_{\text{min}}^2 / \text{dof} = 1.27$.

We present the observational $H(z)$ data with error bars, and the theoretical lines for Λ CDM (solid line) and Int Λ CDM (dashed line) models with the corresponding best-fit parameters in the left panel of Fig. 2.

In the spatially flat XCDM model, the Hubble parameter is

$$H(z) = H_0 \sqrt{\Omega_{m0}(1+z)^3 + (1 - \Omega_{m0})(1+z)^{3(1+w_X)}}, \quad (12)$$

where w_X is the time-independent EoS of dark energy. By minimizing the corresponding χ^2 , we find that the best-fit values for model parameters are $\Omega_{m0} = 0.284$ and $w_X = -0.899$, while $\chi_{\text{min}}^2 = 9.02$ and $\chi_{\text{min}}^2 / \text{dof} = 1.29$.

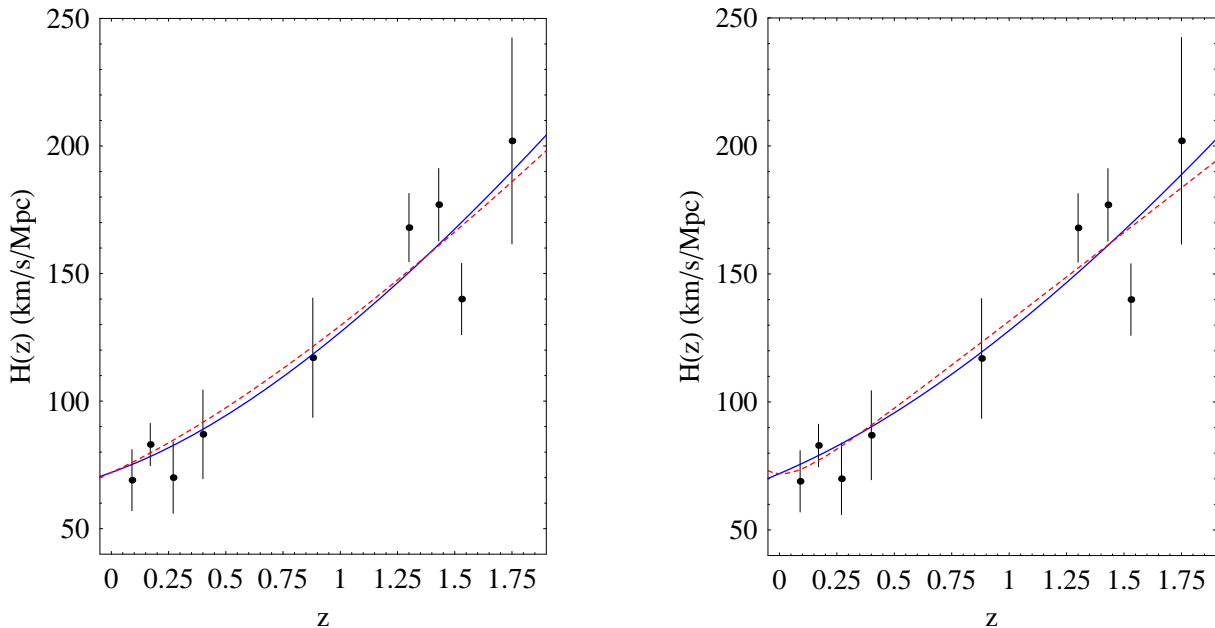


Figure 2: The observational $H(z)$ data with error bars, and the theoretical lines for Λ CDM (left panel) and XCDM (right panel) models with the corresponding best-fit parameters for the cases without (blue solid line) and with (red dashed line) interaction, respectively.

Next, we consider the interacting XCDM model (IntXCDM). In this case, Eq. (3) reads

$$\dot{\rho}_X + 3H(1 + w_X)\rho_X = -3\alpha H\rho_m. \quad (13)$$

Considering Eq. (6), we obtain

$$\rho_X = \text{const.} \cdot a^{-3(1+w_X)} - \frac{\alpha\rho_{m0}}{\alpha + w_X} a^{-3(1-\alpha)}, \quad (14)$$

where *const.* is an integral constant. Again, inserting it into the Friedmann equation $H^2 = \kappa^2(\rho_m + \rho_X)/3$ and requiring $H(z=0) = H_0$, we can determine this integral constant. Finally, in the IntXCDM model, the Hubble parameter is written as

$$H(z) = H_0 \sqrt{\frac{w_X \Omega_{m0}}{\alpha + w_X} (1+z)^{3(1-\alpha)} + \left(1 - \frac{w_X \Omega_{m0}}{\alpha + w_X}\right) (1+z)^{3(1+w_X)}}. \quad (15)$$

By minimizing the corresponding χ^2 , we find that the best-fit values for model parameters are $\Omega_{m0} = 0.718$, $w_X = -3.705$ and $\alpha = 0.302$, while $\chi_{min}^2 = 8.48$ and $\chi_{min}^2/dof = 1.41$.

We present the observational $H(z)$ data with error bars, and the theoretical lines for XCDM (solid line) and IntXCDM (dashed line) models with the corresponding best-fit parameters in the right panel of Fig. 2.

It can be seen clearly from Fig. 2 that none of the above four models may reproduce the sharp dip around $z \sim 1.5$; the data point near $z \sim 1.5$ deviates from model fitting by about 2σ .

3 Vector-like dark energy

As mentioned in the introduction, we are interested to seek a cosmological model whose effective EoS can cross -1 . In this section, we consider the (interacting) vector-like dark energy model proposed in [28] (see also [16]). In this model, the EoS of vector-like dark energy and then the effective EoS can cross -1 in principle. From [16, 28], the energy density and pressure of vector-like dark energy are given by

$$\rho_A = \frac{3}{2} (\dot{A} + HA)^2 + 3V(A^2), \quad (16)$$

$$p_A = \frac{1}{2} (\dot{A} + HA)^2 - 3V(A^2) + 2\frac{dV}{dA^2}A^2, \quad (17)$$

where $A^2(t)$ is the time-dependent length of the so-called ‘‘cosmic triad’’ of three mutually orthogonal vector fields. In this work, we would like to consider the case with exponential potential, namely

$$V(A^2) = V_A \exp(-\lambda\kappa^2 A^2), \quad (18)$$

where V_A and λ are constants. By using Eq. (6) and new quantities $B \equiv \kappa A$ and $\tilde{V}_A \equiv \kappa^2 V_A$, we can recast Eq. (3) as

$$\left(\dot{B} + HB\right) \left[\ddot{B} + 3H\dot{B} + \left(\dot{H} + 2H^2\right)B - 2\lambda\tilde{V}_A B e^{-\lambda B^2}\right] = -3\alpha H H_0^2 \Omega_{m0}(1+z)^{3(1-\alpha)}. \quad (19)$$

To find the solution for $B(t)$, we can use the initial conditions

$$B_{ini} = \pm \sqrt{\frac{2(\lambda-1)}{\lambda}}, \quad \dot{B}_{ini} = 0, \quad (20)$$

which come from [16], under the conditions $\lambda > 1$ and $\alpha < 1$. It is convenient to change the time t to redshift z , and

$$\dot{f} = -(1+z)Hf', \quad (21)$$

$$\ddot{f} = (1+z)H^2 f' - (1+z)\dot{H}f' + (1+z)^2 H^2 f'', \quad (22)$$

where $f' \equiv df/dz$ for any function f ; we have used Eq. (2). From the Raychaudhuri equation $\dot{H} = -\kappa^2(\rho_A + \rho_m + p_A)/2$, we get the \dot{H} in Eq. (22) as

$$\dot{H} = -[-(1+z)B' + B]^2 H^2 + \lambda\tilde{V}_A B^2 e^{-\lambda B^2} - \frac{3}{2}H_0^2 \Omega_{m0}(1+z)^{3(1-\alpha)}. \quad (23)$$

From the Friedmann equation, the Hubble parameter reads

$$H = H_0 \sqrt{\Omega_{m0}(1+z)^{3(1-\alpha)} + \frac{\kappa^2 \rho_A}{3H_0^2}}.$$

Inserting Eq. (16) into it, we find

$$H^2 = \frac{H_0^2 \Omega_{m0}(1+z)^{3(1-\alpha)} + \tilde{V}_A e^{\lambda B^2}}{1 - \frac{1}{2}[-(1+z)B' + B]^2}. \quad (24)$$

From Eq. (24) and the requirement of $H(z=0) = H_0$, only three of α , λ , Ω_{m0} and \tilde{V}_A are independent of each other. We choose our free model parameters as α , λ and Ω_{m0} .

Now, we can numerically solve Eqs. (19) and (20) with the help of Eqs. (21)–(24) to get the $B(z)$. Then, we obtain the Hubble parameter $H(z)$ from Eq. (24). So, the corresponding χ^2 is in hand.

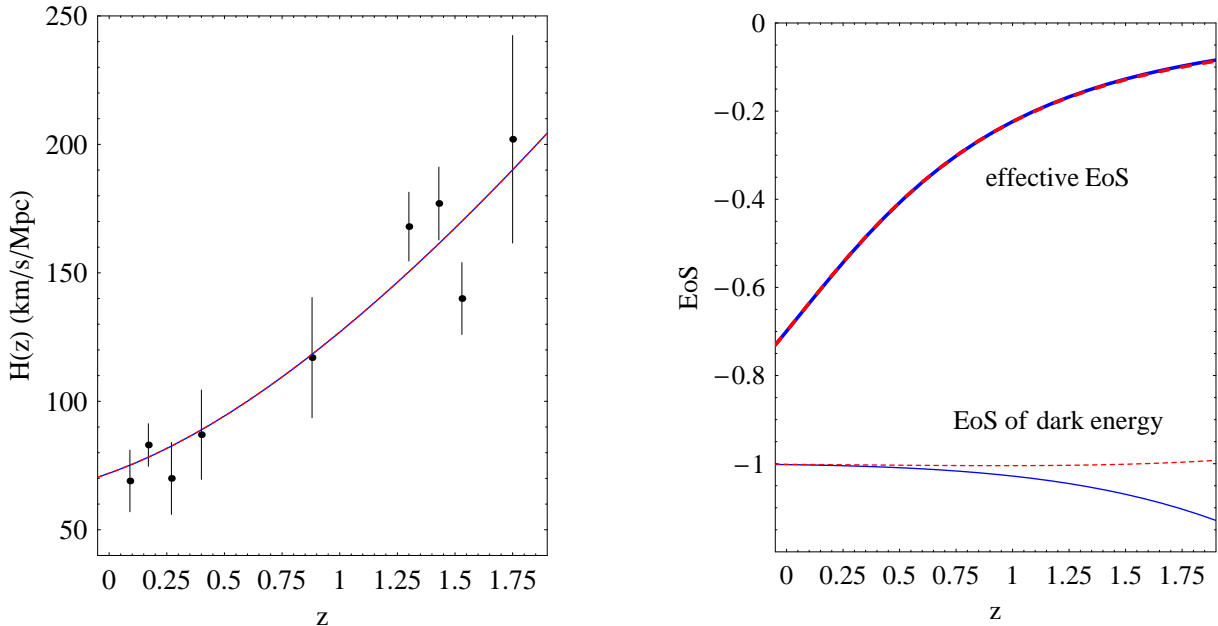


Figure 3: The left panel is the observational $H(z)$ data with error bars, and the theoretical lines for VecDE (blue solid line) and IntVecDE (red dashed line) models with the corresponding best-fit parameters. The right panel shows the effective EoS (thick lines) and the EoS of vector-like dark energy (thin lines), for VecDE (blue solid line) and IntVecDE (red dashed line) models.

For the vector-like dark energy model without interaction (VecDE), i.e. $\alpha = 0$ exactly, we find the minimal χ^2 as $\chi_{min}^2 = 9.05$ ($\chi_{min}^2/dof = 1.29$), for the best-fit parameters $\lambda = 1.001$ and $\Omega_{m0} = 0.299$ (the corresponding $\tilde{V}_A = 0.70 H_0^2$).

For the interacting vector-like dark energy model (IntVecDE), i.e. leaving α as a free parameter, we find the minimal χ^2 as $\chi_{min}^2 = 9.04$ ($\chi_{min}^2/dof = 1.51$), for the best-fit parameters $\alpha = -0.002$, $\lambda = 1.005$ and $\Omega_{m0} = 0.30$ (the corresponding $\tilde{V}_A = 0.703 H_0^2$).

We present the observational $H(z)$ data with error bars, and the theoretical lines for VecDE and IntVecDE models with the corresponding best-fit parameters in the left panel of Fig. 3. The right panel of Fig. 3 shows their corresponding effective EoS and the EoS of vector-like dark energy.

We see that the $H(z)$ predicted by VecDE and IntVecDE models, and their corresponding effective EoS, cannot be clearly distinguished. Also, it can be seen clearly from Fig. 3 that none of these two models may reproduce the sharp dip around $z \sim 1.5$; the data point near $z \sim 1.5$ deviates from model fitting by about 2σ . Although the EoS of vector-like dark energy for VecDE and IntVecDE models are different, they have not crossed -1 . We will briefly discuss this point in section 5.

4 The models with oscillating $H(z)$ ansatz

Obviously, all six models studied above fail to catch the features of the sharp dip around $z \sim 1.5$ and EoS crossing -1 mentioned in the introduction. In this section, we consider some parameterized models.

The first parameterized model (OA1) is the best model studied in [29] which fits the SNe Ia data very well. Its Hubble parameter is given by

$$H(z) = H_0 \sqrt{\Omega_{m0}(1+z)^3 + a_1 \cos(a_2 z^2 + a_3) + (1 - a_1 \cos a_3 - \Omega_{m0})}, \quad (25)$$

where a_1 , a_2 and a_3 are constants. By minimizing the corresponding χ^2 for the $H(z)$ data, we find that the best-fit values for model parameters are $\Omega_{m0} = 0.241$, $a_1 = 1.316$, $a_2 = 2.717$ and $a_3 = -3.933$, while $\chi_{min}^2 = 4.27$ and $\chi_{min}^2/dof = 0.85$.

Adding interaction into it, we obtain the IntOA1 model with Hubble parameter

$$H(z) = H_0 \sqrt{\Omega_{m0}(1+z)^{3(1-\alpha)} + a_1 \cos(a_2 z^2 + a_3) + (1 - a_1 \cos a_3 - \Omega_{m0})}, \quad (26)$$

We find that the best-fit values for model parameters are $\Omega_{m0} = 1.002$, $\alpha = 0.407$, $a_1 = -1.419$, $a_2 = 2.995$ and $a_3 = -1.366$, while $\chi_{min}^2 = 3.54$ and $\chi_{min}^2/dof = 0.89$.

We present the observational $H(z)$ data with error bars, and the theoretical lines for OA1 and IntOA1 models with the corresponding best-fit parameters in the left panel of Fig. 4. The right panel of Fig. 4 shows the effective EoS,

$$w_{eff} \equiv \frac{p_{tot}}{\rho_{tot}} = -1 + \frac{2}{3}(1+z) \frac{H'}{H}, \quad (27)$$

for OA1 and IntOA1 models, respectively. It is obvious that both effective EoS of OA1 and IntOA1 models crossed -1 . The $H(z)$ lines predicted by these two models dip around $z \sim 1.5$. So, it is not surprising that they fit the observational $H(z)$ data much better than the six models studied above.

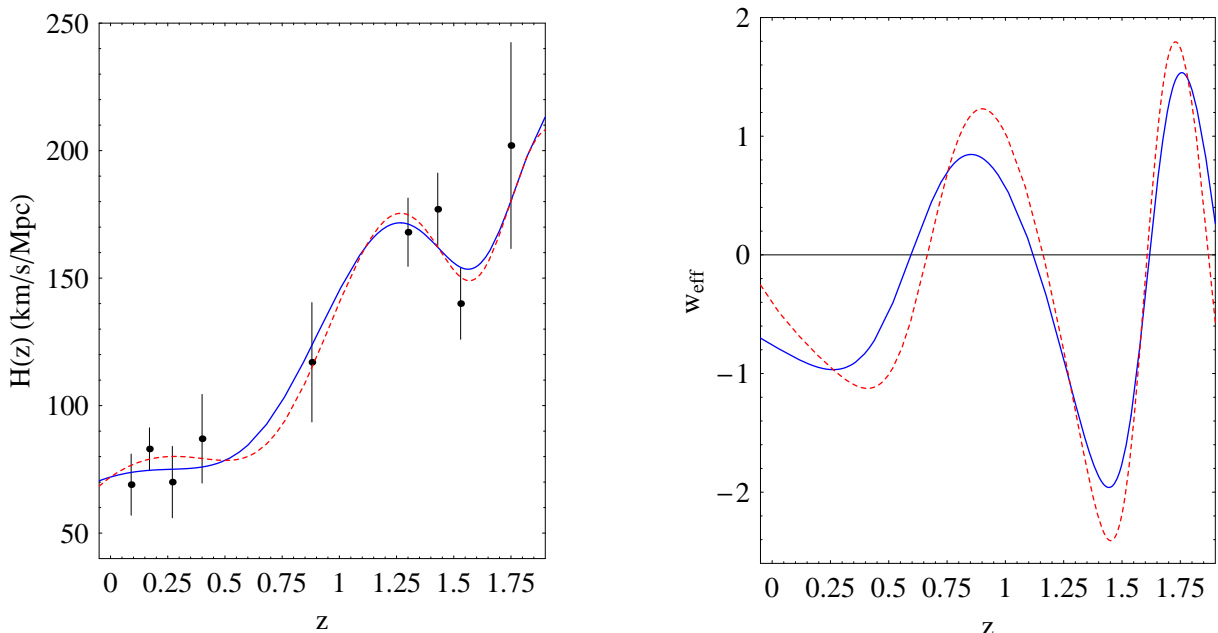


Figure 4: The left panel is the observational $H(z)$ data with error bars, and the theoretical lines for OA1 (blue solid line) and IntOA1 (red dashed line) models with the corresponding best-fit parameters. The right panel shows their corresponding effective EoS.

Next, we consider a variant (OA2) of the best model studied in [30] which also fits the SNe Ia data very well. Its Hubble parameter reads

$$H(z) = H_0 \sqrt{\Omega_{m0}(1+z)^3 + a_1(1+z)^3 [\cos(a_2 z^2 + a_3) - \cos a_3] + (1 - \Omega_{m0})}, \quad (28)$$

where a_1 , a_2 and a_3 are constants. By minimizing the corresponding χ^2 , we find that the best-fit values for model parameters are $\Omega_{m0} = 0.287$, $a_1 = 0.132$, $a_2 = 2.971$ and $a_3 = -4.481$, while $\chi_{min}^2 = 2.81$ and $\chi_{min}^2/dof = 0.56$.

We get the IntOA2 model by adding interaction into OA2. The corresponding Hubble parameter is given by

$$H(z) = H_0 \sqrt{\Omega_{m0}(1+z)^{3(1-\alpha)} + a_1(1+z)^{3(1-\alpha)} [\cos(a_2 z^2 + a_3) - \cos a_3] + (1 - \Omega_{m0})}. \quad (29)$$

We find that the best-fit values for model parameters are $\Omega_{m0} = 0.252$, $\alpha = -0.048$, $a_1 = -0.117$, $a_2 = 2.975$ and $a_3 = -1.351$, while $\chi_{min}^2 = 2.80$ and $\chi_{min}^2/dof = 0.70$.

We present the observational $H(z)$ data with error bars, and the theoretical lines for OA1 and IntOA1 models with the corresponding best-fit parameters in the left panel of Fig. 5. The right panel of Fig. 5 shows their corresponding effective EoS. Again, we see the OA2 and IntOA2 models catch the main features of the observational $H(z)$ data; they reproduce the sharp dip around $z \sim 1.5$ and their effective EoS crossed -1 also. Since the value of α is too small, there is no significant difference between OA2 and IntOA2 models, unlike the case of OA1 and IntOA1 models.

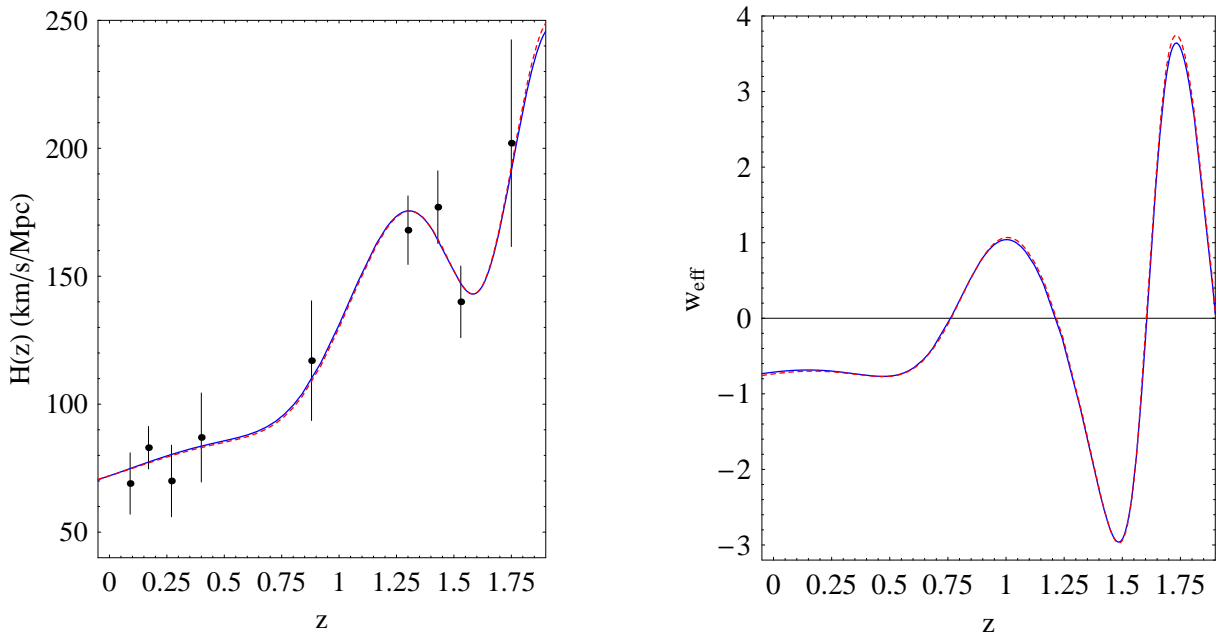


Figure 5: The left panel is the observational $H(z)$ data with error bars, and the theoretical lines for OA2 (blue solid line) and IntOA2 (red dashed line) models with the corresponding best-fit parameters. The right panel shows their corresponding effective EoS.

5 Concluding remarks

In Table 2, we summarize all ten models considered in this work. It is obvious that they divide into two groups. The first six models fail to catch the main features of the observational $H(z)$ data, and hence have large χ_{min}^2 and χ_{min}^2/dof . The last four models with oscillating $H(z)$ ansatz, on the contrary, are well compatible with the observational $H(z)$ data. They can reproduce the sharp dip around $z \sim 1.5$, and their effective EoS crossed -1 also. Therefore, it is not surprising that their corresponding χ_{min}^2 and χ_{min}^2/dof are significantly smaller than the ones of the first six models.

Model	χ_{min}^2	χ_{min}^2/dof	$P(\chi^2 > \chi_{min}^2)$	Ranked by $P(\chi^2 > \chi_{min}^2)$
Λ CDM	9.04	1.13	0.34	5
Int Λ CDM	8.89	1.27	0.26	6
XCDM	9.02	1.29	0.25	7
IntXCDM	8.48	1.41	0.21	9
VecDE	9.05	1.29	0.25	8
IntVecDE	9.04	1.51	0.17	10
OA1	4.27	0.85	0.51	3
IntOA1	3.54	0.89	0.47	4
OA2	2.81	0.56	0.73	1
IntOA2	2.80	0.70	0.59	2

Table 2: Summarizing all ten models considered in this work.

Some remarks are in order. The first one is on the failure of the vector-like dark energy model to reproduce the main features of the observational $H(z)$ data, since the EoS of vector-like dark energy and then the effective EoS can cross -1 in principle. According to [16], for the case of interaction term $C = 3\alpha H\rho_m$, the vector-like dark energy behaves like a pure cosmological constant in the late time. So, it is not surprising that the vector-like dark energy model considered in this work is very close to the Λ CDM model. However, when the interaction term C takes other forms, the late time behavior of vector-like dark energy can be considerably different, as shown explicitly in [16]. Therefore, it is interesting to compare the observational $H(z)$ data with the interacting vector-like dark energy model with other interaction forms and different potentials. We leave this to future works.

Secondly, we note that the best-fit value $\Omega_{m0} = 1.002$ of IntOA1 model is inconsistent with the results from clusters of galaxies [38] and 3-year WMAP [3] etc. In this sense, the IntOA1 model may be ruled out, although it fits the observational $H(z)$ data fairly well.

The third remark is concerned with EoS crossing -1 . There are many pieces of other observational evidence for this in the literature [30, 31, 32, 33]. Also, a lot of theoretical models whose EoS can cross -1 have been built (see for examples [16, 17, 24, 32, 34, 40] and references therein). In this work, we present independent evidence for EoS crossed -1 , from the observational $H(z)$ data.

Fourthly, we see that the last four models fit the data much better than the first six models. We note that the last four models have an oscillating feature, for both predicted $H(z)$ and EoS, as shown in Figs. 4 and 5. In fact, this is also the main ideas of [35, 36, 37, 41]. However, the last four models studied here and the ones considered in [35, 36, 37, 41] are all *parameterized* models. We consider that it is important to build some physically motivated models in which the oscillating EoS arises naturally.

Fifthly, we admit that although the first six models have considerably larger χ_{min}^2/dof , they are not unacceptable. For instance, the Λ CDM model has $\chi_{min}^2 = 9.04$ for eight degrees of freedom with 34% probability, which is not unacceptably low. Also, before the new and improved $H(z)$ data are available, it is too early to talk about *strong observational evidence* for non-monotonic behavior of $H(z)$, since one can wonder that the dip around $z \sim 1.5$ could be due to unknown measurement errors and so on. Therefore, to firmly rule out non-oscillating models (e.g. the first six models considered here), the more and better observational $H(z)$ data are required.

Finally, the observational $H(z)$ data provide an independent approach to constrain the cosmological models. However, by now, the observational $H(z)$ data only have 9 data points and their error bars are fairly large. Hence, they cannot severely constrain the cosmological models so far. A good news from [15] is that a large amount of $H(z)$ data is expected to become available in the next few years. These include data from the AGN and Galaxy Survey (AGES) and the Atacama Cosmology Telescope (ACT), and by 2009 an order of magnitude increase in $H(z)$ data is anticipated.

Acknowledgments

We thank Lado Samushia and Raul Jimenez for useful communications. We are grateful to Professor Rong-Gen Cai for helpful discussions. We also thank Hui Li, Xin Zhang, Meng Su, and Nan Liang, Rong-Jia Yang, Wei-Ke Xiao, Jun-Zheng Li, Yuan Liu, Xiao Che, Fu-Yan Bian for kind help and discussions. We acknowledge partial funding support by the Ministry of Education of China, Directional Research Project of the Chinese Academy of Sciences and by the National Natural Science Foundation of China under project No. 10521001.

References

- [1] A. G. Riess *et al.* [Supernova Search Team Collaboration], *Astron. J.* **116**, 1009 (1998) [astro-ph/9805201];
S. Perlmutter *et al.* [Supernova Cosmology Project Collaboration], *Astrophys. J.* **517**, 565 (1999) [astro-ph/9812133];
J. L. Tonry *et al.* [Supernova Search Team Collaboration], *Astrophys. J.* **594**, 1 (2003) [astro-ph/0305008];
R. A. Knop *et al.*, [Supernova Cosmology Project Collaboration], *Astrophys. J.* **598**, 102 (2003) [astro-ph/0309368];
A. G. Riess *et al.* [Supernova Search Team Collaboration], *Astrophys. J.* **607**, 665 (2004) [astro-ph/0402512].
- [2] P. Astier *et al.* [SNLS Collaboration], *Astron. Astrophys.* **447**, 31 (2006) [astro-ph/0510447];
J. D. Neill *et al.* [SNLS Collaboration], astro-ph/0605148.
- [3] C. L. Bennett *et al.* [WMAP Collaboration], *Astrophys. J. Suppl.* **148**, 1 (2003) [astro-ph/0302207];
D. N. Spergel *et al.* [WMAP Collaboration], *Astrophys. J. Suppl.* **148** 175 (2003) [astro-ph/0302209];
D. N. Spergel *et al.* [WMAP Collaboration], astro-ph/0603449;
L. Page *et al.* [WMAP Collaboration], astro-ph/0603450;
G. Hinshaw *et al.* [WMAP Collaboration], astro-ph/0603451;
N. Jarosik *et al.* [WMAP Collaboration], astro-ph/0603452.

- [4] M. Tegmark *et al.* [SDSS Collaboration], Phys. Rev. D **69**, 103501 (2004) [astro-ph/0310723];
M. Tegmark *et al.* [SDSS Collaboration], Astrophys. J. **606**, 702 (2004) [astro-ph/0310725];
U. Seljak *et al.*, Phys. Rev. D **71**, 103515 (2005) [astro-ph/0407372];
J. K. Adelman-McCarthy *et al.* [SDSS Collaboration], Astrophys. J. Suppl. **162**, 38 (2006)
[astro-ph/0507711];
K. Abazajian *et al.* [SDSS Collaboration], astro-ph/0410239; astro-ph/0403325; astro-ph/0305492;
M. Tegmark *et al.* [SDSS Collaboration], astro-ph/0608632.
- [5] S. W. Allen, R. W. Schmidt, H. Ebeling, A. C. Fabian and L. van Speybroeck, Mon. Not. Roy. Astron. Soc. **353**, 457 (2004) [astro-ph/0405340].
- [6] P. J. E. Peebles and B. Ratra, Rev. Mod. Phys. **75**, 559 (2003) [astro-ph/0207347];
T. Padmanabhan, Phys. Rept. **380**, 235 (2003) [hep-th/0212290];
S. M. Carroll, astro-ph/0310342;
R. Bean, S. Carroll and M. Trodden, astro-ph/0510059;
V. Sahni and A. A. Starobinsky, Int. J. Mod. Phys. D **9**, 373 (2000) [astro-ph/9904398];
S. M. Carroll, Living Rev. Rel. **4**, 1 (2001) [astro-ph/0004075];
T. Padmanabhan, Curr. Sci. **88**, 1057 (2005) [astro-ph/0411044];
S. Weinberg, Rev. Mod. Phys. **61**, 1 (1989);
S. Nobbenhuis, gr-qc/0411093;
E. J. Copeland, M. Sami and S. Tsujikawa, hep-th/0603057;
R. Trotta and R. Bower, astro-ph/0607066.
- [7] R. Jimenez and A. Loeb, Astrophys. J. **573**, 37 (2002) [astro-ph/0106145].
- [8] R. Jimenez, L. Verde, T. Treu and D. Stern, Astrophys. J. **593**, 622 (2003) [astro-ph/0302560].
- [9] J. Simon, L. Verde and R. Jimenez, Phys. Rev. D **71**, 123001 (2005) [astro-ph/0412269].
- [10] R. G. Abraham *et al.* [GDDS Collaboration], Astron. J. **127**, 2455 (2004) [astro-ph/0402436].
- [11] T. Treu, M. Stiavelli, S. Casertano, P. Moller and G. Bertin, Mon. Not. Roy. Astron. Soc. **308**, 1037 (1999);
T. Treu, M. Stiavelli, P. Moller, S. Casertano and G. Bertin, Mon. Not. Roy. Astron. Soc. **326**, 221 (2001) [astro-ph/0104177];
T. Treu, M. Stiavelli, S. Casertano, P. Moller and G. Bertin, Astrophys. J. Lett. **564**, L13 (2002);
J. Dunlop, J. Peacock, H. Spinrad, A. Dey, R. Jimenez, D. Stern and R. Windhorst, Nature **381**, 581 (1996);
H. Spinrad, A. Dey, D. Stern, J. Dunlop, J. Peacock, R. Jimenez and R. Windhorst, Astrophys. J. **484**, 581 (1997);
L. A. Nolan, J. S. Dunlop, R. Jimenez and A. F. Heavens, Mon. Not. Roy. Astron. Soc. **341**, 464 (2003) [astro-ph/0103450].
- [12] Z. L. Yi and T. J. Zhang, astro-ph/0605596, MPLA in press.
- [13] N. Pires, Z. H. Zhu and J. S. Alcaniz, Phys. Rev. D **73**, 123530 (2006) [astro-ph/0606689].
- [14] M. A. Dantas, J. S. Alcaniz, D. Jain and A. Dev, astro-ph/0607060.
- [15] L. Samushia and B. Ratra, Astrophys. J. **650**, L5 (2006) [astro-ph/0607301].

- [16] H. Wei and R. G. Cai, Phys. Rev. D **73**, 083002 (2006) [astro-ph/0603052].
- [17] H. Wei, R. G. Cai and D. F. Zeng, Class. Quant. Grav. **22**, 3189 (2005) [hep-th/0501160];
H. Wei and R. G. Cai, Phys. Rev. D **72**, 123507 (2005) [astro-ph/0509328];
M. Alimohammadi and H. Mohseni Sadjadi, Phys. Rev. D **73**, 083527 (2006) [hep-th/0602268];
W. Zhao and Y. Zhang, Phys. Rev. D **73**, 123509 (2006) [astro-ph/0604460].
- [18] A. A. Coley, gr-qc/9910074;
J. Wainwright and G. F. R. Ellis, *Dynamical Systems in Cosmology*, Cambridge Univ. Press, Cambridge, 1997;
A. A. Coley, *Dynamical Systems and Cosmology*, in Series: Astrophysics and Space Science Library, Vol. 291, Springer, 2004.
- [19] E. J. Copeland, A. R. Liddle and D. Wands, Phys. Rev. D **57**, 4686 (1998) [gr-qc/9711068].
- [20] L. Amendola, Phys. Rev. D **60**, 043501 (1999) [astro-ph/9904120];
L. Amendola, Phys. Rev. D **62**, 043511 (2000) [astro-ph/9908023];
L. Amendola and C. Quercellini, Phys. Rev. D **68**, 023514 (2003) [astro-ph/0303228];
L. Amendola and D. Tocchini-Valentini, Phys. Rev. D **64**, 043509 (2001) [astro-ph/0011243];
L. Amendola and D. Tocchini-Valentini, Phys. Rev. D **66**, 043528 (2002) [astro-ph/0111535];
L. Amendola, C. Quercellini, D. Tocchini-Valentini and A. Pasqui, Astrophys. J. **583**, L53 (2003) [astro-ph/0205097].
- [21] Z. K. Guo, R. G. Cai and Y. Z. Zhang, JCAP **0505**, 002 (2005) [astro-ph/0412624];
Z. K. Guo and Y. Z. Zhang, Phys. Rev. D **71**, 023501 (2005) [astro-ph/0411524].
- [22] T. Damour and A. M. Polyakov, Nucl. Phys. B **423**, 532 (1994) [hep-th/9401069];
T. Damour and A. M. Polyakov, Gen. Rel. Grav. **26**, 1171 (1994) [gr-qc/9411069];
C. Wetterich, Astron. Astrophys. **301**, 321 (1995) [hep-th/9408025];
J. R. Ellis, S. Kalara, K. A. Olive and C. Wetterich, Phys. Lett. B **228**, 264 (1989);
G. Huey, P. J. Steinhardt, B. A. Ovrut and D. Waldram, Phys. Lett. B **476**, 379 (2000) [hep-th/0001112];
C. T. Hill and G. G. Ross, Nucl. Phys. B **311**, 253 (1988);
G. W. Anderson and S. M. Carroll, astro-ph/9711288;
B. Gunjudpai, T. Naskar, M. Sami and S. Tsujikawa, JCAP **0506**, 007 (2005) [hep-th/0502191].
- [23] H. Wei and R. G. Cai, Phys. Rev. D **71**, 043504 (2005) [hep-th/0412045].
- [24] H. Wei and R. G. Cai, astro-ph/0607064.
- [25] W. Zimdahl, D. Pavon and L. P. Chimento, Phys. Lett. B **521**, 133 (2001) [astro-ph/0105479];
L. P. Chimento, A. S. Jakubi, D. Pavon and W. Zimdahl, Phys. Rev. D **67**, 083513 (2003) [astro-ph/0303145].
- [26] R. G. Cai and A. Wang, JCAP **0503**, 002 (2005) [hep-th/0411025];
E. Majerotto, D. Sapone and L. Amendola, astro-ph/0410543.
- [27] W. L. Freedman *et al.*, Astrophys. J. **553**, 47 (2001) [astro-ph/0012376].
- [28] C. Armendariz-Picon, JCAP **0407**, 007 (2004) [astro-ph/0405267].

- [29] S. Nesseris and L. Perivolaropoulos, *Phys. Rev. D* **70**, 043531 (2004) [astro-ph/0401556].
- [30] R. Lazkoz, S. Nesseris and L. Perivolaropoulos, *JCAP* **0511**, 010 (2005) [astro-ph/0503230].
- [31] D. Huterer and A. Cooray, *Phys. Rev. D* **71**, 023506 (2005) [astro-ph/0404062];
 U. Alam, V. Sahni and A. A. Starobinsky, *JCAP* **0406**, 008 (2004) [astro-ph/0403687];
 Y. Wang and M. Tegmark, *Phys. Rev. D* **71**, 103513 (2005) [astro-ph/0501351];
 S. Nesseris and L. Perivolaropoulos, *Phys. Rev. D* **70**, 043531 (2004) [astro-ph/0401556];
 B. A. Bassett, P. S. Corasaniti and M. Kunz, *Astrophys. J.* **617**, L1 (2004) [astro-ph/0407364];
 Y. Wang and P. Mukherjee, astro-ph/0604051;
 A. Cabre, E. Gaztanaga, M. Manera, P. Fosalba and F. Castander, astro-ph/0603690.
- [32] B. Feng, X. L. Wang and X. M. Zhang, *Phys. Lett. B* **607**, 35 (2005) [astro-ph/0404224].
- [33] J. Q. Xia, G. B. Zhao, B. Feng, H. Li and X. M. Zhang, *Phys. Rev. D* **73**, 063521 (2006) [astro-ph/0511625];
 J. Q. Xia, G. B. Zhao, B. Feng and X. M. Zhang, astro-ph/0603393;
 G. B. Zhao, J. Q. Xia, B. Feng and X. M. Zhang, astro-ph/0603621;
 J. Q. Xia, G. B. Zhao, H. Li, B. Feng and X. M. Zhang, astro-ph/0605366;
 J. Q. Xia, G. B. Zhao and X. M. Zhang, astro-ph/0609463.
- [34] H. Wei and R. G. Cai, *Phys. Lett. B* **634**, 9 (2006) [astro-ph/0512018].
 Z. K. Guo, Y. S. Piao, X. M. Zhang and Y. Z. Zhang, *Phys. Lett. B* **608**, 177 (2005) [astro-ph/0410654];
 Z. K. Guo, Y. S. Piao, X. M. Zhang and Y. Z. Zhang, astro-ph/0608165;
 X. Zhang and F. Q. Wu, *Phys. Rev. D* **72**, 043524 (2005) [astro-ph/0506310];
 X. Zhang, *Int. J. Mod. Phys. D* **14**, 1597 (2005) [astro-ph/0504586];
 X. F. Zhang, H. Li, Y. S. Piao and X. M. Zhang, *Mod. Phys. Lett. A* **21**, 231 (2006) [astro-ph/0501652];
 Y. F. Cai, H. Li, Y. S. Piao and X. M. Zhang, gr-qc/0609039.
- [35] B. Feng, M. Z. Li, Y. S. Piao and X. M. Zhang, *Phys. Lett. B* **634**, 101 (2006) [astro-ph/0407432].
- [36] S. Nojiri and S. D. Odintsov, *Phys. Lett. B* **637**, 139 (2006) [hep-th/0603062].
- [37] E. V. Linder, *Astropart. Phys.* **25**, 167 (2006) [astro-ph/0511415].
- [38] For examples, S. Borgani, astro-ph/0605575;
 S. Borgani *et al.*, *Astrophys. J.* **561**, 13 (2001) [astro-ph/0106428];
 J. P. Henry, *Astrophys. J.* **609**, 603 (2004) [astro-ph/0404142].
- [39] M. Szydlowski, *Phys. Lett. B* **632**, 1 (2006) [astro-ph/0502034];
 M. Szydlowski, T. Stachowiak and R. Wojtak, *Phys. Rev. D* **73**, 063516 (2006) [astro-ph/0511650].
- [40] M. Z. Li, B. Feng and X. M. Zhang, *JCAP* **0512**, 002 (2005) [hep-ph/0503268];
 Z. Chang, F. Q. Wu and X. Zhang, *Phys. Lett. B* **633**, 14 (2006) [astro-ph/0509531];
 H. S. Zhang and Z. H. Zhu, *Phys. Rev. D* **73**, 043518 (2006) [astro-ph/0509895].
- [41] G. Barenboim, O. Mena and C. Quigg, *Phys. Rev. D* **71**, 063533 (2005) [astro-ph/0412010].